PFC/JA-91-26

Effect of Longitudinal Space–Charge Waves of a Helical Relativistic Electron Beam on the Cyclotron Maser Instability

Chen, C.; Danly, B.G.; Shvets, G.; Wurtele, J.S.

Plasma Fusion Center
Massachusetts Institute of Technology
Cambridge, MA 02139

September 1991

This work was supported by DE–FG02–91ER–40648, DOE Chicago, IL.

Submitted to IEEE Transactions on Plasma Science

Effect of Longitudinal Space-Charge Waves of a Helical Relativistic Electron Beam on the Cyclotron Maser Instability

C. Chen, B.G. Danly, G. Shvets, and J.S. Wurtele
Plasma Fusion Center
Massachusetts Institute of Technology
Cambridge, Massachusetts 02139

ABSTRACT

The influence of the longitudinal space-charge waves of a coherently gyrophased, helical relativistic electron beam on the cyclotron maser instability is investigated in a cylindrical waveguide configuration using a three-dimensional kinetic theory. A dispersion relation that includes waveguide effects is derived. The stability properties of the cyclotron maser interaction are examined in detail. It is shown that, in general, the effects of space-charge waves on a coherently gyrophased beam are suppressed in a waveguide geometry in comparison with an ideal one-dimensional cyclotron maser with similar beam parameters.

I. INTRODUCTION

It is well-known that in ideal one-dimensional systems the longitudinal electrostatic waves of an isotropically gyrophased relativistic electron beam decouple from the co-propagating transverse electromagnetic waves in a uniform magnetic field. The interaction of the fast electromagnetic wave and the beam cyclotron mode, driven by an inverted population in the perpendicular momentum of the electron distribution function $f_0(p_\perp^2, p_z)$, leads to the cyclotron maser instability [1],[2], providing the physical mechanism for coherent radiation generation in relativistic cyclotron autoresonance masers [3]-[8] and gyrotrons [3],[9].

In the early 1970's, Kotsarenko *et al* [10] realized that both space-charge waves and beam cyclotron modes can interact with the fast electromagnetic wave, provided that the initial distribution of the electron gyrophases is nonuniform or coherent. An example of such a coherently gyrophased beam is a helical beam that is often transformed from a solid beam by means of a wiggler or kicker magnet [6]-[8]. Recently, Fruchtman and Friedland developed a one-dimensional linear theory using both a cold-fluid model [11] and a kinetic model [12]. Kho *et al* [13] subsequently performed one-dimensional computer simulations and found good agreement with the kinetic theory. These analyses concluded that the longitudinal space-charge waves can strongly alter the stability properties of the cyclotron maser interaction. In particular, near the cyclotron resonance, the growth rate for a coherently gyrophased beam was found to be substantially larger than that for an isotropically gyrophased beam. Also, Antonsen *et al* [14] investigated the effects of transverse space-charge waves in gyrotrons.

In this paper, a three-dimensional kinetic theory is developed describing the interaction of the longitudinal space-charge waves on a coherently gyrophased, helical relativistic electron beam with the beam cyclotron and transverse-electric (TE) waveguide modes in a cylindrical waveguide geometry. A dispersion relation that includes waveguide boundary conditions is derived. The detailed stability properties of the cyclotron maser interaction are eximined. In comparison with the existing one-dimensional theory [12],[13], the results of this paper show that the presence of a waveguide plays an important role in suppressing longitudinal space-charge wave effects.

The basic physical mechanism for the excitation of longitudinal space-charge-waves in the cyclotron maser (with $k_{\|} \neq 0$) driven by a coherently gyrophased electron beam is similar to that in the free-electron laser [2] in the sense that there is a ponderomotive force bunching the electrons axially in configuration space. The ponderomotive force results from the beating between transverse electromagnetic perturbations and the coherent modulation of the electron transverse velocities induced by the wiggler magnetic field in the free-electron laser or by the axial magnetic field in the cyclotron maser. However, in the cyclotron maser, coherent velocity modulations occur only when the distribution of the electron gyrophases at the entrance of the interaction ($z = 0$) is coherent, e.g., a delta function distribution where all particles have the same gyrophase.

The organization of this paper is as follows. After presenting the basic equations and assumptions in Sec. II, a dispersion relation is derived in Sec. III for the cyclotron maser interaction including longitudinal space-charge waves and waveguide effects. The dispersion relation is analyzed in Sec. IV.

II. BASIC EQUATIONS AND ASSUMPTIONS

We consider a relativistic electron beam undergoing cyclotron motion in an applied uniform magnetic field $B_0\vec{e}_z$ and propagating axially through a lossless cylindrical waveguide of radius r_w. The motion of each individual electron is described by the Lorentz force equation

$$\frac{d\vec{p}}{dt} = -e\left[\delta\vec{E} + \frac{\vec{v}}{c} \times (B_0\vec{e}_z + \delta\vec{B})\right] , \tag{1}$$

and the electron phase-space density function $f(\vec{x}, \vec{p}, t)$ evolves according to the Vlasov equation

$$\frac{\partial f}{\partial t} + \vec{v} \cdot \frac{\partial f}{\partial \vec{x}} - e\Big[\delta\vec{E} + \frac{\vec{v}}{c} \times (B_0 \vec{e}_z + \delta\vec{B})\Big] \cdot \frac{\partial f}{\partial \vec{p}} = 0 \,. \tag{2}$$

In Eqs. (1) and (2), $-e$ is the electron charge, c is the speed of light *in vacuo*, and the perturbed electric and magnetic fields, $\delta\vec{E}(\vec{x}, t)$ and $\delta\vec{B}(\vec{x}, t)$, include electromagnetic and space-charge wave contributions.

A. Equilibrium State

In the absence of perturbations ($\delta\vec{E} = 0 = \delta\vec{B}$), the exact constants of motion for an individual electron in the applied magnetic field $B_0\vec{e}_z$ are the electron guiding-center radius and angle, r_g and θ_g, the perpendicular and axial momentum components, $p_\perp = (p_x^2 + p_y^2)^{1/2}$ and p_z, and the quantity $\phi - m_0\Omega_c z/p_z$, where m_0 is the electron rest mass, $\Omega_c = eB_0/m_0c$ is the nonrelativistic cyclotron frequency, and $\phi = \tan^{-1}(p_y/p_x)$ is the gyrophase of the electron (see Fig. 1). Therefore, the equilibrium distribution function describing a cold, coherently gyrophased relativistic electron beam can be expressed as

$$f_0(r_g, \phi - m_0\Omega_c z/p_z, p_\perp, p_z) = \frac{n_b}{p_{\perp 0}} G(r_g)\delta(p_\perp - p_{\perp 0})\delta(p_z - p_{z0})\delta\Big(\phi - \frac{m_0\Omega_c z}{p_z}\Big) \,, \tag{3}$$

with $\int G(r_g) r_g dr_g d\theta_g = 1$, $r_g = [r^2 + r_L^2 + 2rr_L \sin(\theta - \phi)]^{1/2}$, and $r_L = p_\perp/m_0\Omega_c$. In Eq. (3), n_b is the number of electrons per unit axial length and δ is the delta function. The electron density in cylindrical coordinates is given by

$$n(r, \theta, z) = \int f_0(r_g, \phi - m_0\Omega_c/p_z, p_\perp, p_z) p_\perp dp_\perp dp_z d\phi = n_b G(\bar{r}_g(r, \theta, z)) \,, \tag{4}$$

where $\bar{r}_g(r, \theta, z) = [r^2 + r_L^2 + 2rr_L \sin(\theta - m_0\Omega_c z/p_{z0})]^{1/2}$, and $r_L = p_{\perp 0}/m_0\Omega_c$ is the Larmor radius of the electron with $p_\perp = p_{\perp 0}$. The density $n(r, \theta, z)$ has an axial periodicity of $L = 2\pi p_{z0}/m_0\Omega_c = 2\pi\gamma v_z/\Omega_c$. The remainder of this analysis assumes an on-axis helical electron beam with

$$G(r_g) = \begin{cases} 1/\pi r_{gm}^2 & \text{if } 0 \le r_g < r_{gm} \ll r_w \\ 0 & \text{if } r_g > r_{gm} \ . \end{cases} \tag{5}$$

B. Field Perturbations

In principle, the periodic equilibrium state f_0 supports electromagnetic and space-charge wave perturbations of a Floquet type. In the present analysis, however, we assume that only one Floquet component in the radiation field, namely, a transverse-electric (TE_{mn}) mode, can strongly couple to the electron beam and space-charge waves. The electric and magnetic fields of the TE_{mn} mode are [4],[5]

$$\delta \vec{E}_t(\vec{x}, t) = \frac{1}{2}\delta E_{mn}\vec{e}_z \times \nabla_t \Psi_{mn}(r, \theta) \exp[i(k_\parallel z - \omega t)] + \text{c.c.} \ , \tag{6}$$

$$\delta \vec{B}_t(\vec{x}, t) = -\frac{1}{2}\frac{ck_\parallel}{\omega}\delta E_{mn}\nabla_t \Psi_{mn}(r, \theta) \exp[i(k_\parallel z - \omega t)] + \text{c.c.} \ , \tag{7}$$

$$\delta B_z(\vec{x}, t) = \frac{1}{2}\frac{ick_{mn}^2}{\omega}\delta E_{mn}\Psi_{mn}(r, \theta) \exp[i(k_\parallel z - \omega t)] + \text{c.c.} \ , \tag{8}$$

where $\nabla_t = \vec{e}_r\partial/\partial r + (\vec{e}_\theta/r)\partial/\partial\theta$, the subscript t denotes the transverse components of the electromagnetic perturbation, δE_{mn} is the amplitude of the TE_{mn} mode, and $\omega = 2\pi f$ is the (angular) frequency of the perturbation. The vacuum TE_{mn} eigenfunction is defined by

$$\Psi_{mn}(r, \theta) = C_{mn} J_m(k_{mn} r) \exp(im\theta) \ , \tag{9}$$

with $k_{mn}^2/C_{mn}^2 = \pi(\nu_{mn}^2 - m^2)J_m^2(\nu_{mn})$. Here, $J_m(x)$ is the Bessel function of first kind of order m, and $\nu_{mn} = k_{mn}r_w$ is the nth zero of $J_m'(x) = dJ_m(x)/dx$. The function Ψ_{mn} satisfies the eigenvalue equation

$$(\nabla_t^2 + k_{mn}^2)\Psi_{mn}(r,\theta) = 0 \ , \tag{10}$$

the boundary condition $\partial\Psi_{mn}(r = r_w, \theta)/\partial r = 0$, and the normalization condition $\int_{\pi r_w^2} \Psi_{mn}^* \Psi_{mn} d\sigma = 1$.

To further simplify the analysis, we assume that the space-charge wave is *longitudinal* and radially symmetric ($\partial/\partial\theta = 0$). Under this assumption, the space-charge-wave field is approximately electrostatic and given by

$$\delta\vec{E}^{(sc)}(\vec{x},t) = \delta E_z^{(sc)}(\vec{x},t)\vec{e}_z = \frac{1}{2}\delta E^{(sc)}C^{(sc)}J_0(k_\perp^{(sc)}r)\exp[i(k_\parallel^{(sc)}z - \omega t)]\vec{e}_z + \text{c.c.} \ . \tag{11}$$

[The magnetic and transverse electric fields associated with the space-charge wave are of order $J_1(k_\perp^{(sc)}r) \sim k_\perp^{(sc)}r_{gm} \ll 1$.] In Eq. (11), $k_\perp^{(sc)} = \mu/r_w$ is the transverse wave number of the space-charge wave, $J_0(\mu) = 0$, and $C^{(sc)} = k_\perp^{(sc)}/\pi^{1/2}\mu J_0'(\mu)$ is a normalization factor. The wave number of the space-charge wave, $k_\parallel^{(sc)}$, remains to be determined [see Eq. (40)].

C. Wave Equations

From the Maxwell's equations, it can be shown that the electromagnetic perturbation satisfies the wave equation

$$\left(\frac{d^2}{dz^2} + \nabla_t^2 + \frac{\omega^2}{c^2}\right)\delta\vec{B} = -\frac{4\pi}{c}\nabla \times \delta\vec{J} \ , \tag{12}$$

that the space-charge wave satisfies the continuity-Poisson equation

$$\frac{\partial \delta E_z^{(sc)}}{\partial t} = -4\pi \delta J_z \ . \tag{13}$$

In Eqs. (12) and (13), the current density perturbation is

$$\delta \vec{J}(\vec{x}, t) = -e \int \vec{v} f_1(\vec{x}, \vec{p}, t) d\vec{p} \ , \tag{14}$$

with $f_1(\vec{x}, \vec{p}, t) = f(\vec{x}, \vec{p}, t) - f_0(r_g, \phi - m_0\Omega_c/p_z, p_\perp, p_z)$.

Substituting Eqs. (6)-(8) and (14) into Eq. (12), multiplying the equation by Ψ^*_{mn}, and integrating over the cross section of the waveguide yields

$$\left(\frac{\omega^2}{c^2} - k_\parallel^2 - k_{mn}^2\right)\delta E_{mn} = \frac{8\pi i e\omega}{c^2 k_{mn}^2} \int d\vec{p} d\sigma (\vec{e}_z \times \nabla_t \Psi^*_{mn}) \cdot \vec{v} f_1 \exp[-i(k_\parallel z - \omega t)] \tag{15}$$

for the TE_{mn} mode. Similarly, from Eqs. (11), (13) and (14), we have

$$\delta E^{(sc)} = \frac{8\pi i e}{\omega} \int d\vec{p} d\sigma C^{(sc)} J_0(k_\perp^{(sc)} r) v_z f_1 \exp[-i(k_\parallel^{(sc)} z - \omega t)] \tag{16}$$

for the space-charge wave.

D. Linearized Vlasov Equation

The electron phase-space density perturbation $f_1(\vec{x}, \vec{p}, t)$ evolves according to the linearized Vlasov equation

$$v_z \frac{df_1}{dz} \equiv \frac{\partial f_1}{\partial t} + \vec{v} \cdot \frac{\partial f_1}{\partial \vec{x}} - \frac{e}{c}(\vec{v} \times B_0 \vec{e}_z) \cdot \frac{\partial f_1}{\partial \vec{p}} = e\left(\delta \vec{E} + \frac{\vec{v}}{c} \times \delta \vec{B}\right) \cdot \frac{\partial f_0}{\partial \vec{p}} \ . \tag{17}$$

In Eq. (17), the usual total time derivative is replaced by total derivative with respect to the axial distance z because the system has a single frequency and it is the spatial evolution of the perturbation that is of interest. Furthermore, it is convenient to express Eq. (17) in terms of the guiding-center phase-space variables $(r_g, \theta_g, z, p_\perp, \phi, p_z)$ illustrated in Fig. 1. Using $\delta\vec{E} = \delta E_\perp \vec{e}_\perp + \delta E_\phi \vec{e}_\phi + \delta E_z^{(sc)} \vec{e}_z$ and $\delta\vec{B} = \delta B_\perp \vec{e}_\perp + \delta B_\phi \vec{e}_\phi + \delta B_z \vec{e}_z$ with $\vec{e}_\perp = \vec{e}_r \cos(\phi - \theta) + \vec{e}_\theta \sin(\phi - \theta)$ and $\vec{e}_\phi = -\vec{e}_r \sin(\phi - \theta) + \vec{e}_\theta \cos(\phi - \theta)$, some straightforward algebraic manipulations result in

$$\frac{v_z}{e}\frac{df_1}{dz} = (\delta E_\perp - \beta_z \delta B_\phi)\frac{\partial f_0}{\partial p_\perp} + \beta_\perp \delta B_\phi \frac{\partial f_0}{\partial p_z} + \delta E_z^{(sc)} \frac{\partial f_0}{\partial p_z} , \tag{18}$$

where $\beta_\perp = v_\perp/c$, $\beta_z = v_z/c$. The partial derivatives with respect to $p_\perp$ and p_z are defined in the independent guiding-center phase-space variables,

$$\frac{1}{f_0}\frac{\partial f_0}{\partial p_\perp} = \frac{\delta'(p_\perp - p_{\perp 0})}{\delta(p_\perp - p_{\perp 0})} \tag{19}$$

and

$$\frac{1}{f_0}\frac{\partial f_0}{\partial p_z} = \frac{\delta'(p_z - p_{z0})}{\delta(p_z - p_{z0})} + \frac{m_0 \Omega_c z}{p_z^2}\frac{\delta'(\phi - m_0\Omega_c z/p_z)}{\delta(\phi - m_0\Omega_c z/p_z)} . \tag{20}$$

In Eq. (18), we have neglected the terms proportional to $G'(r_g)$ and $\partial f_0/\partial\phi$. Inclusion of these terms would add terms of order $(\omega - k_\parallel v_z - l\Omega_c/\gamma)^{-1}$ to the dispersion relation [Eq. (42)], and not change our basic conclusions.

III. DISPERSION RELATION

To derive the dispersion relation, we make use of recurrence relations and Graf's theorem for Bessel functions [15] to express the field perturbations in Eq. (18) as

$$\delta E_\perp = \delta E_r \cos(\phi - \theta) + \delta E_\theta \sin(\phi - \theta)$$

$$= \frac{1}{2} k_{mn} C_{mn} \delta E_{mn} \sum_{l=-\infty}^{\infty} X_{mnl}(r_g, r_L) \exp[i\Lambda_{ml}(z, \phi, \theta_g, t)] + \text{c.c.} \ , \tag{21}$$

$$\delta E_z^{(sc)} = \frac{1}{2} C^{(sc)} \delta E^{(sc)} \sum_{l=\infty}^{\infty} X_l^{(sc)}(r_g, r_L) \exp[i\Lambda_l^{(sc)}(z, \phi, \theta_g, t)] + \text{c.c.} \ , \tag{22}$$

$$\delta B_\phi = \frac{ck_\parallel}{\omega} \delta E_\perp \ . \tag{23}$$

Here,

$$\Lambda_{ml}(z, \phi, \theta_g, t) = k_\parallel z - \omega t + l\phi - (l-m)\theta_g + (l-2m)\pi/2 \ , \tag{24}$$

$$\Lambda_l^{(sc)}(z, \phi, \theta_g, t) = k_\parallel^{(sc)} z - \omega t + l\phi - l\theta_g + l\pi/2 \ , \tag{25}$$

$$X_{mnl}(r_g, r_L) = J_{l-m}(k_{mn} r_g) J_l'(k_{mn} r_L) \ , \tag{26}$$

$$X_l^{(sc)}(r_g, r_L) = J_l(k_\perp^{(sc)} r_g) J_l(k_\perp^{(sc)} r_L) \ . \tag{27}$$

Substituting Eqs. (21)-(23) into Eq. (18) yields

$$\begin{aligned} \frac{df_1}{dz} = \frac{e}{2v_z} k_{mn} C_{mn} \delta E_{mn} \Big[\sum_{l=-\infty}^{\infty} X_{mnl} \exp(i\Lambda_{ml}) \Big] \Big[\Big(1 - \frac{k_\parallel v_z}{\omega}\Big) \frac{\partial f_0}{\partial p_\perp} + \frac{k_\parallel v_\perp}{\omega} \frac{\partial f_0}{\partial p_z} \Big] \\ + \frac{e}{2v_z} C^{(sc)} \delta E^{(sc)} \Big[\sum_{l=-\infty}^{\infty} X_l^{(sc)} \exp(i\Lambda_l^{(sc)}) \Big] \frac{\partial f_0}{\partial p_z} + \text{c.c.} \ , \end{aligned} \tag{28}$$

Integrating Eq. (28) along the characteristics given by $t(z') = t + (z'-z)/v_z$ and $\phi(z') = \phi + (\Omega_c/\gamma)(z'-z)/v_z$, we find

$$f_1 = f_1^{(+)} + \text{c.c.} \,, \tag{29}$$

$$f_1^{(+)}(r_g, \theta_g, z, p_\perp, p_z, \phi, t)$$
$$= \frac{e}{2i} \sum_{l=-\infty}^{\infty} \left\{ \frac{k_{mn} C_{mn} X_{mnl} \delta E_{mn} \exp(i\Lambda_{ml})}{k_\| v_z - \omega + l\Omega_c/\gamma} O_l^{TE} + \frac{C^{(sc)} X_l^{(sc)} \delta E^{(sc)} \exp(i\Lambda_l^{(sc)})}{k_\|^{(sc)} v_z - \omega + l\Omega_c/\gamma} O_l^{(sc)} \right\} f_0 \,. \tag{30}$$

The operators O, O_l^{TE}, and $O_l^{(sc)}$ are defined by

$$O = \left(1 - \frac{k_\| v_z}{\omega}\right) \frac{\partial}{\partial p_\perp} + \frac{k_\| v_\perp}{\omega} \frac{\partial}{\partial p_z} \,, \tag{31}$$

$$O_l^{TE} = O + \frac{i v_z}{k_\| v_z - \omega + l\Omega_c/\gamma} \frac{k_\| v_\perp}{\omega} \frac{m_0 \Omega_c}{p_z^2} \frac{\partial}{\partial \phi} \,, \tag{32}$$

and

$$O_l^{(sc)} = \frac{\partial}{\partial p_z} + \frac{i v_z}{k_\|^{(sc)} v_z - \omega + l\Omega_c/\gamma} \frac{m_0 \Omega_c}{p_z^2} \frac{\partial}{\partial \phi} \,. \tag{33}$$

Substituting Eq. (30) into the wave equation (15), and expanding $\Psi_{mn}(r, \theta)$ in terms of guiding-center variables [as used in Eq. (21)], we obtain

$$D_{mn}^{TE}(\omega, k_\|) \delta E_{mn} = \chi(\omega, k_\|^{(sc)}) \delta E^{(sc)} \,, \tag{34}$$

where

$$D_{mn}^{TE}(\omega, k_\|) = \frac{\omega^2}{c^2} - k_\|^2 - k_{mn}^2 - 4\pi e^2 \left(\frac{\omega}{c}\right) C_{mn}^2 \sum_{l=-\infty}^{\infty} \int d\sigma d\vec{p} \frac{\beta_\perp X_{mnl}^2 O f_0}{k_\| v_z - \omega + l\Omega_c/\gamma} \,, \tag{35}$$

$$\chi(\omega, k_\parallel^{(sc)}) = 4\pi e^2 \left(\frac{\omega}{c}\right)\left(\frac{C_{mn}}{k_{mn}}\right) C^{(sc)}$$
$$\times \sum_{l=-\infty}^{\infty} \int d\sigma d\vec{p} \exp[i(\Lambda_{l-m}^{(sc)} - \Lambda_{ml})] \frac{\beta_\perp X_{l-m}^{(sc)} X_{mnl} O_{l-m}^{(sc)} f_0}{k_\parallel^{(sc)} v_z - \omega + (l-m)\Omega_c/\gamma} \ . \tag{36}$$

Similarly, combining Eqs. (16) and (30), we have

$$D^L(\omega, k_\parallel^{(sc)}) \delta E^{(sc)} = \kappa(\omega, k_\parallel) \delta E_{mn} \ , \tag{37}$$

where

$$D^L(\omega, k_\parallel^{(sc)}) = 1 - 4\pi e^2 \left(\frac{c}{\omega}\right)[C^{(sc)}]^2 \sum_{l=-\infty}^{\infty} \int d\sigma d\vec{p} \frac{\beta_z [X_{l-m}^{(sc)}]^2}{k_\parallel^{(sc)} v_z - \omega + (l-m)\Omega_c/\gamma} \frac{\partial f_0}{\partial p_z} \ , \tag{38}$$

$$\kappa(\omega, k_\parallel) = 4\pi e^2 \left(\frac{c}{\omega}\right) k_{mn} C_{mn} C^{(sc)}$$
$$\times \sum_{l=-\infty}^{\infty} \int d\sigma d\vec{p} \exp[i(\Lambda_{ml} - \Lambda_{l-m}^{(sc)})] \frac{\beta_z X_{l-m}^{(sc)} X_{mnl} O_l^{TE} f_0}{k_\parallel v_z - \omega + l\Omega_c/\gamma} \ . \tag{39}$$

To determine the coupling of the TE_{mn} mode and the space-charge wave, we need to evaluate the overlap integrals in Eqs. (36) and (39). After a careful inspection of the integrals, we find that the relation,

$$k_\parallel^{sc} = k_\parallel + m\frac{m_0 \Omega_c}{p_{z0}} \equiv k_\parallel + m\frac{\Omega_c}{\gamma v_z} \ , \qquad m = 1, 2, 3, ..., \tag{40}$$

must be satisfied for the coupling. From Eqs. (35) and (38), we obtain the dispersion relation

$$D_{mn}^{TE}(\omega, k_\parallel) D^L(\omega, k_\parallel^{sc}) = \chi(\omega, k_\parallel^{(sc)}) \kappa(\omega, k_\parallel) \tag{41}$$

with $k_{\parallel}^{(sc)}$ defined in Eq. (40). This dispersion relation can be used to examine the stability properties of the cyclotron maser interaction of a fundamental or harmonic beam cyclotron mode with longitudinal space-charge waves and various TE modes.

In particular, for the cold, coherently gyrophased helical electron beam described in Eqs. (3) and (5), to leading order in $(\omega - k_{\parallel}v_z - l\Omega_c/\gamma)^{-2}$, the dispersion relation (41) for $l = m$ becomes

$$D_{mn}^{TE}(\omega, k_{\parallel})D^{L}(\omega, k_{\parallel}) = \epsilon_{mnl}\epsilon_{l-m}^{(sc)}k_{mn}^{2}(ck_{\perp}^{(sc)})^{2}\frac{(\beta_z\omega - ck_{\parallel})^2}{\Delta_l^4} \, . \tag{42}$$

The dielectric functions for the TE_{mn} mode and the longitudinal space-charge wave, $D_{mn}^{TE}(\omega, k_{\parallel})$ and $D^{L}(\omega, k_{\parallel})$, are given by

$$D_{mn}^{TE}(\omega, k_{\parallel}) = \frac{\omega^2}{c^2} - k_{\parallel}^2 - k_{mn}^2 + \epsilon_{mnl}k_{mn}^2\frac{(\omega^2 - c^2k_{\parallel}^2)}{\Delta_l^2} \tag{43}$$

and

$$D^{L}(\omega, k_{\parallel}) = 1 - \frac{\epsilon_{l-m}^{(sc)}}{\gamma_z^2}\frac{(ck_{\perp}^{(sc)})^2}{\Delta_l^2} \, , \tag{44}$$

respectively. Moreover, $\Delta_l = \omega - k_{\parallel}v_z - l\Omega_c/\gamma$, $\gamma = [1 + (p_{z0}^2 + p_{\perp 0}^2)/m_0^2c^2]^{1/2}$, $\gamma_z = (1 - \beta_z^2)^{-1/2}$, $\beta_{\perp} = v_{\perp}/c = p_{\perp 0}/\gamma m_0 c$, and $\beta_z = v_z/c = p_{z0}/\gamma m_0 c$. Finally, the dimensionless coupling constants ϵ_{mnl} and $\epsilon_{l-m}^{(sc)}$ are defined by

$$\epsilon_{mnl} = \frac{4\beta_{\perp}^2}{\gamma\beta_z}\left(\frac{I_b}{I_A}\right)\frac{[J_{l-m}(k_{mn}r_g)J_l'(k_{mn}r_L)]^2}{(\nu_{mn}^2 - m^2)J_m^2(\nu_{mn})} \tag{45}$$

and

$$\epsilon_{l-m}^{(sc)} = \frac{4}{\gamma\beta_z}\left(\frac{I_b}{I_A}\right)\left[\frac{J_{l-m}(k_\perp^{(sc)}r_g)J_{l-m}(k_\perp^{(sc)}r_L)}{k_\perp^{(sc)}r_w J_0'(k_\perp^{(sc)}r_w)}\right]^2 , \quad (46)$$

respectively. In Eqs. (45) and (46), $I_b = en_b\beta_z c$ is the beam current, and $I_A = m_0c^3/e \cong$ 17 kA, the Alfvén current. The dispersion relation (42) is a six-order polynomial of $k_\|$ and therefore has six solutions for $k_\|$. Each solution with negative imaginary part corresponds to an unstable mode with a spatial growth rate of $-\mathrm{Im}k_\| > 0$.

Three remarks on the dispersion relation (42) are in order. First, the coupling between the longitudinal space-charge wave and the TE_{mn} mode is proportional to $(\beta_z\omega - ck_\|)^2$, which is in agreement with the cold-fluid treatment of Kotsarenko *et al* [10]. This quantity can be negligibly small in waveguide configurations. In fact, at grazing incidence $\beta_z \cong \beta_\phi^{-1} \equiv ck_\|/\omega$, it almost vanishes and therefore space-charge-wave effects are expected to be negligible. In any case, the influence of longitudinal space-charge waves is suppressed due to $k_{mn} \neq 0$ and $\beta_\phi > 1$ in a waveguide geometry. On the contrary, in an ideal one-dimensional system in free space, because $\omega \cong ck_\| = ck$ for electromagnetic waves propagating in the z direction, $(\beta_z\omega - ck_\|)^2 \cong (1-\beta_z)^2\omega^2$. The space-charge waves can then strongly modify the cyclotron maser interaction.

Second, the three-dimensional dispersion relation (42) recovers, to leading order in $(\omega - kv_z - \Omega_c/\gamma)^{-2}$, the corresponding one-dimensional dispersion relation [12],[13] with the following substitutions

$$l \to 1 \ , \ \ k_\| \to k \ , \ \ k_{mn} \to 0 \ , \ \ \epsilon_{l-m}^{(sc)}(ck_\perp^{(sc)})^2 \to \frac{\omega_{pb}^2}{\gamma} \ , \ \ \epsilon_{mnl}^{(sc)}(ck_{mn})^2 \to \frac{\omega_{pb}^2}{\gamma}\left(\frac{\beta_\perp^2}{2}\right) . \quad (47)$$

Here, $\omega_{pb} = (4\pi e^2 n_e/m_0)^{1/2}$ is the nonrelativistic plasma frequency associated with a constant electron density of n_e in the one-dimensional theory.

Third, in the case of an isotropically gyrophased electron beam with an unperturbed distribution function depending on $p_\perp$ and p_z but not on $\phi - m_0\Omega_c z/p_z$, it can be shown that the space-charge wave decouples from the TE$_{mn}$ mode with $m \neq 0$, that the dispersion relation (42) reduces to

$$D^{TE}_{mn}(\omega, k_\|) = 0 \ , \qquad m, n = 1, 2, 3, ... \tag{48}$$

for the TE$_{mn}$ mode, and

$$D^L(\omega, k_\|) = 0 \tag{49}$$

for the space-charge wave. However, the space-charge wave does couple to the TE$_{0n}$ mode, though the interaction is not a cyclotron maser type. In this case, the dispersion relation is shown to be the same as Eq. (42) with $m = l = 0$.

IV. NUMERICAL RESULTS

In this section, the dispersion relation (42) is analyzed to illustrate the effect of the longitudinal space-charge wave on the cyclotron maser interaction in a cylindrical waveguide configuration for the coherently gyrophased, helical relativistic electron beam described in Eqs. (3) and (5). The results are compared with the corresponding isotropically gyrophased beam as well as with the corresponding coherently gyrophased beam in an ideal one-dimensional system.

Figure 2 shows the gain bandwidth of the TE$_{11}$ mode for the following choice of system parameters: beam current $I_b = 500$ A, beam energy $\gamma = 4.0$, normalized perpendicular velocity $\beta_\perp = 0.36$, $l = 1$, axial magnetic field $B_0 = 18.94$ kG, waveguide radius $r_w = 0.3$ cm, $r_{gm} \approx 0$, $k_\perp^{(sc)} = \mu/r_w = 2.405/r_w$, and $k_{11} = \nu_{11}/r_w = 1.8412/r_w$. In Fig. 2, the solid curve shows the spatial growth rate, $-\mathrm{Im}k_\|$, as a function of frequency calculated from Eq. (42) for the coherently gyrophased electron beam, while the dashed curve shows the spatial growth rate calculated from Eq. (48) for the isotropically gyrophased electron beam.

Several interesting features are illustrated in Fig. 2. First, it is evident that inclusion of the space-charge wave broadens the gain bandwidth of the fast unstable TE_{11} mode (corresponding to the dashed curve in the frequency range from $\omega/ck_{11} = 1.2$ to 4.2). Similar behavior has been found in ideal one-dimensional systems [12],[13]. Second, the influence of the space-charge wave on the cyclotron maser interaction is small, particularly near the cyclotron resonant frequencies $\omega/ck_{11} \cong 3.24$ (or $\omega/2\pi \cong 95$ GHz) and $\omega/ck_{11} \cong 1.5$ (or $\omega/2\pi \cong 44$ GHz). This is because the cyclotron maser interaction is the most unstable near the cyclotron resonance in waveguide configurations and waveguide effects play an important role in suppressing the longitudinal space-charge wave, as it was discussed in Sec. III. In contrast, for an ideal one-dimensional system, the longitudinal space-charge wave of the corresponding coherently gyrophased beam results in strong instability at the exact cyclotron resonance [12],[13], i.e., the autoresonance, where there is little gain for the corresponding isotropically gyrophased beam [1],[2]. Third, space-charge wave effects cause instability in the frequency range from $\omega/ck_{11} \cong 4.2$ to 4.5, where the net axial and inertial bunching vanish in the case of the isotropically gyrophased beam [5],[16].

Figure 3 shows the gain bandwidth for a coherently and an isotropically gyrophased electron beam corresponding to the gyro-TWT amplifier experiment conducted at the Naval Research Laboratory (NRL) [7]. The system parameters are $I_b = 500$ A, $\gamma = 2.76$, $\beta_\perp = 0.4$, $l = 1$, $B_0 = 8.0$ kG, $r_w = 0.54$ cm, $r_{gm} \approx 0$, $k_\perp^{(sc)} = \mu/r_w = 2.405/r_w$, and $k_{11} = \nu_{11}/r_w = 1.8412/r_w$. The amplifier operated near grazing incidence at $\omega/2\pi = 35$ GHz (or $\omega/ck_{11} = 2.01$). Although the bandwidth (solid curve) for the coherently gyrophased beam is wider than the bandwidth (dashed curve) for the isotropically gyrophased beam, there is little difference at the operating frequency $\omega/ck_{11} = 2.01$, where $\beta_z\omega - ck_\parallel \cong 0$

due to grazing incidence. This calculation suggests that the discrepancy [7] between the measured and theoretically predicted growth rates can not be resolved by the inclusion of longitudinal space-charge into the theoretical analysis.

V. CONCLUSIONS

In conclusion, a three-dimensional kinetic theory in a waveguide geometry was developed for the cyclotron maser interaction including the longitudinal, radially symmetric space-charge waves of a coherently gyrophased, helical relativistic electron beam. A dispersion relation was derived and the detailed stability properties of the cyclotron maser interaction were examined. The results were compared with the existing one-dimensional theory [12],[13]. It was shown that, in general, the influence of longitudinal space-charge waves on a coherently gyrophased beam is suppressed in a waveguide geometry in comparison with an ideal one-dimensional cyclotron maser with similar beam parameters. A moderate enhancement of the growth rate was found near the cyclotron resonance for relatively high-current, high-density beams. Moreover, longitudinal space-charge wave effects were shown to be negligibly small near grazing incidence.

ACKNOWLEDGMENTS

The authors wish to thank John Davies for stimulating discussions and assistance in the analysis of the dispersion relation. The authors are also grateful to M.I. Petelin for discussions and pointing out the work by Kotsarenko *et al.* This work was supported by the Office of Basic Energy Sciences and the Division of High Energy Physics of the U.S. Department of Energy.

References

[1] K.R. Chu and J.L. Hirshfield, "Comparative study of the axial and azimuthal bunching mechanisms in electromagnetic cyclotron instabilities," Phys. Fluids, Vol. 21, pp. 461-466, 1978.

[2] R.C. Davidson, *Physics of Nonneutral Plasmas* (Addison-Wesley, Reading, Massachusetts, 1990), Chap. 7.

[3] V.L. Bratman, N.S. Ginzburg, G.S. Nusinovich, M.I. Petelin, and P.S. Strelkov, "Relativistic gyrotrons and cyclotron autoresonance masers," Int. J. Electron., Vol. 51, 541-567, 1981.

[4] A.W. Fliflet, "Linear and non-linear theory of the Doppler-shifted cyclotron resonance maser based on TE and TM waveguide modes," Int. J. Electron., Vol. 61, 1049-1080, 1986.

[5] C. Chen and J.S. Wurtele, "Linear and nonlinear of cyclotron autoresonance masers with multiple waveguide modes," Phys. Fluids, Vol. B3, pp. 2133-2148, 1991, and references therein.

[6] A.C. DiRienzo, G. Bekefi, C. Chen, and J.S. Wurtele, "Experimental and theoretical studies of a 35 GHz cyclotron autoresonance maser amplifier," Phys. Fluids, Vol. B3, pp. 1755-1765, 1991.

[7] S.H. Gold, D.A. Kirkpatrick, A.W. Fliflet, R.B. McCowan, A.K. Kinkead, D.L. Hardesty, and M. Sucy, "High-voltage millimeter-wave gyro-traveling-wave amplifier," J. Appl. Phys., Vol. 69, pp. 6696-6698, 1991.

[8] K.D. Pendergast, D.G. Danly, W.L. Menninger, R.J. Temkin, "Long-pulse cyclotron autoresonance maser oscillator experiment," submitted to IEEE J. Electron. for publication, 1991.

[9] K.E. Kreischer and R.J. Temkin, "Single-mode operation of a high-power step-tunable gyrotron," Phys. Rev. Lett., Vol. 59, pp. 549-550, 1987.

[10] N. Ya. Kotsarenko, V.P. Semik, and A.M. Fedorchenko, "Interaction of cyclotron waves and space-charge waves of a rotating electron beam with fast electromagnetic waves," Radio Eng. Electron. Phys., Vol. 15, pp. 2260-2267, 1970.

[11] A. Fruchtman and L. Friedland, "Amplification of frequency up-shifted radiation by cold relativistic guided electron beams," J. Appl. Phys., Vol. 53, pp. 4011-4015, 1982.

[12] A. Fruchtman and L. Friedland, "Theory of a nonwiggler collective free-electron laser in uniform magnetic field," IEEE J. Quamtum Electron., Vol. 19, pp. 327-333, 1983.

[13] T.H. Kho, A.T. Lin, and L. Chen, "Gyrophase-coherent electron cyclotron maser," Phys. Fluids, Vol. 31, pp. 3120-3126, 1988.

[14] T.M. Antonsen, Jr., W.M. Manheimer, and B. Levush, "Effect of ac and dc transverse self-fields in gyrotrons," Int. J. Electron., Vol. 61, pp. 823-854, 1986.

[15] M. Abramowitz and I.A. Stegun, *Handbook of Mathematical Functions* (Dover, New York, 1972), Chap. 9.

[16] C. Chen and J.S. Wurtele, "Efficiency enhancement in cyclotron autoresonance maser amplifiers by magnetic field tapering," Phys. Rev. A, Vol. 40, pp. 489-492, 1989.

FIGURE CAPTIONS

Fig. 1 Guiding center coordinate system.

Fig. 2 The solid and dashed curves show the gain bandwidth for the cyclotron maser interaction calculated from Eqs. (42) and (48) for coherently and isotropically gyrophased electron beams, respectively. The choice of system parameters corresponds to $I_b = 500$ A, $\gamma = 4.0$, $\beta_\perp = 0.36$, $l = 1$, $B_0 = 18.94$ kG, $r_w = 0.3$ cm, $r_{gm} \approx 0$, $k_\perp^{(sc)} = \mu/r_w = 2.405/r_w$, and $k_{11} = \nu_{11}/r_w = 1.8412/r_w$.

Fig. 3 The solid and dashed curves show the gain bandwidth for the cyclotron maser interaction at grazing incidence for coherently and isotropically gyrophased electron beams, respectively. The choice of system parameters corresponds to the NRL gyro-TWT amplifier experiment: $I_b = 500$ A, $\gamma = 2.76$, $\beta_\perp = 0.4$, $l = 1$, $B_0 = 8.0$ kG, $r_w = 0.54$ cm, $r_{gm} \approx 0$, $k_\perp^{(sc)} = \mu/r_w = 2.405/r_w$, and $k_{11} = \nu_{11}/r_w = 1.8412/r_w$. The operating frequency is 35 GHz or $\omega/ck_{11} = 2.01$.

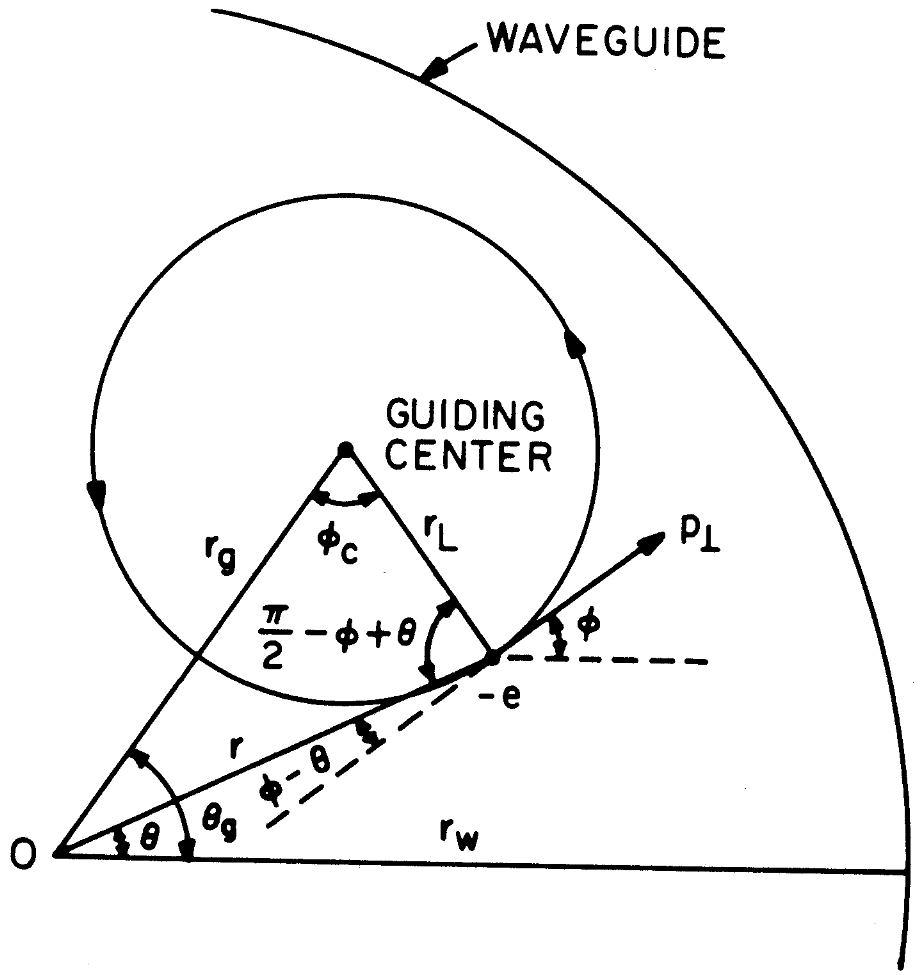
WAVEGUIDE
GUIDING
CENTER
r_g
ϕ_c
r_L
$p_\perp$
$\frac{\pi}{2}-\phi+\theta$
ϕ
$-e$
r
$\phi-\theta$
O
θ
θ_g
r_w

Fig. 1

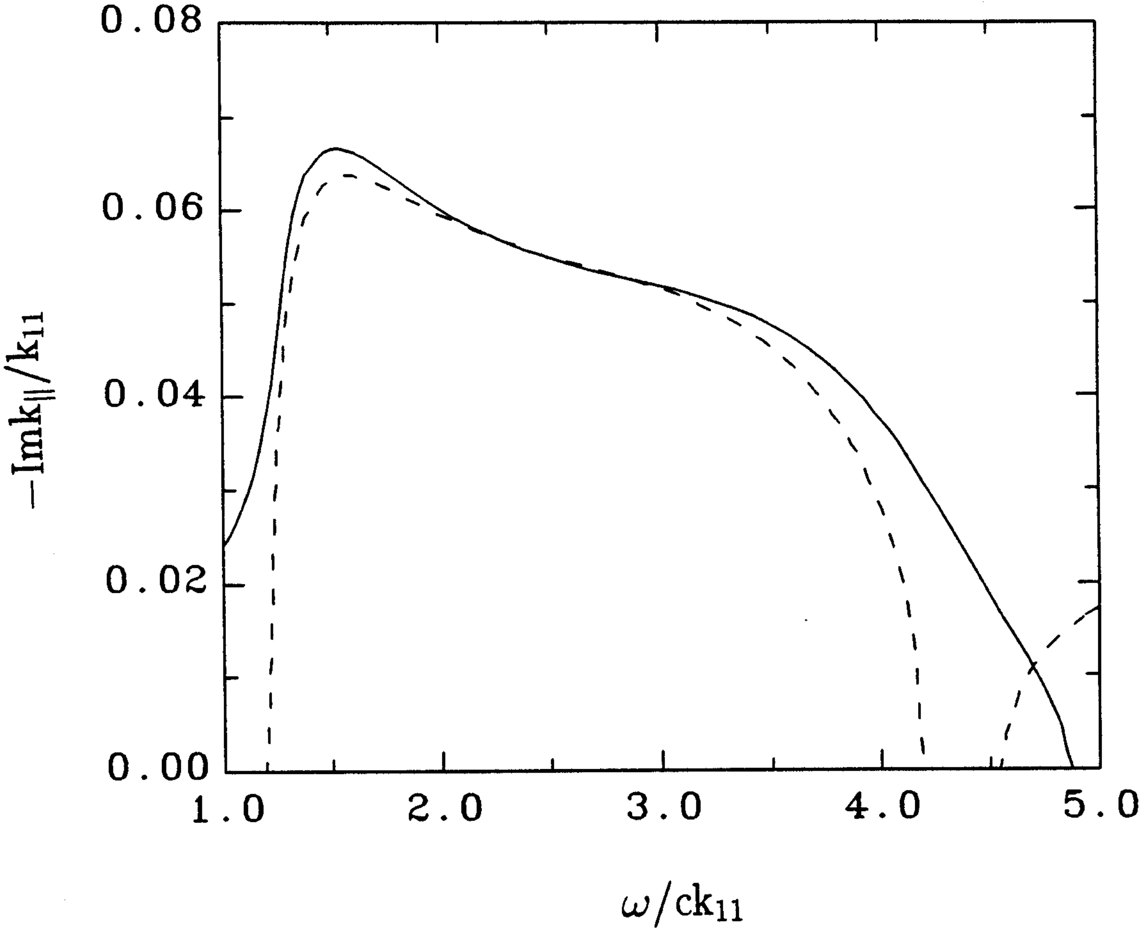

Fig. 2

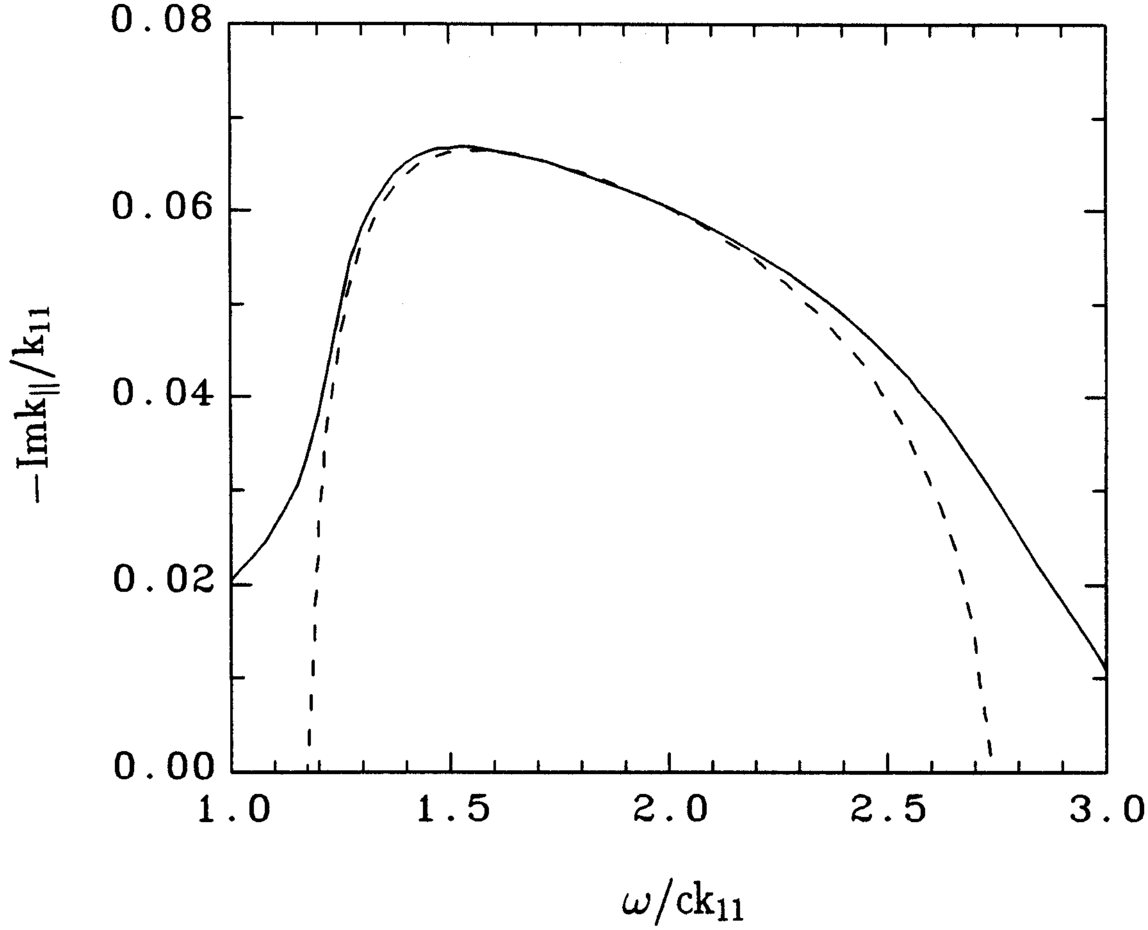
0.08
0.06
0.04
0.02
0.00
1.0
1.5
2.0
2.5
3.0
$-\mathrm{Im}k_{\parallel}/k_{11}$
ω/ck_{11}

Fig. 3